J. Fluid Mech. (1999), *vol.* 389, *pp.* 361–389. Printed in the United Kingdom

On the evolution of non-axisymmetric viscous fibres with surface tension, inertia and gravity

By L. J. CUMMINGS[1]† AND P. D. HOWELL[2]

[1] Faculty of Mathematics, Technion–I.I.T., 32000 Haifa, Israel

[2] Mathematical Institute, 24–29 St Giles', Oxford OX1 3LB, UK

(Received 20 July 1998 and in revised form 26 January 1999)

We consider the free boundary problem for the evolution of a nearly straight slender fibre of viscous fluid. The motion is driven by prescribing the velocity of the ends of the fibre, and the free surface evolves under the action of surface tension, inertia and gravity. The three-dimensional Navier–Stokes equations and free-surface boundary conditions are analysed asymptotically, using the fact that the inverse aspect ratio, defined to be the ratio between a typical fibre radius and the initial fibre length, is small. This first part of the paper follows earlier work on the stretching of a slender viscous fibre with negligible surface tension effects. The inclusion of surface tension seriously complicates the problem for the evolution of the shape of the cross-section. We adapt ideas applied previously to two-dimensional Stokes flow to show that the shape of the cross-section can be described by means of a conformal map which depends on time and distance along the fibre axis. We give some examples of suitable relevant conformal maps and present numerical solutions of the resulting equations. We also use analytic methods to examine the coupling between stretching and the evolution of the cross-section shape.

1. Introduction

There is a large body of literature on the flow of slender viscous jets. Most of the previous work is motivated by the processes of optical or synthetic fibre draw-down, shown schematically in figure 1. Here a liquid fibre is extruded from a nozzle and stretched under the tension applied at its other end. The flow in such a process is typically (i) axisymmetric and (ii) steady, and the emphasis of previous modelling efforts has tended to reflect these properties. Thus, (i) the axisymmetric Navier–Stokes equations (or suitable generalization if the fibre is non-Newtonian) and free-surface conditions are usually taken as a starting point in the analysis, and (ii) time dependence is often only considered when determining the stability or otherwise of a particular steady state. The reader is referred to Howell (1994) for a more comprehensive overview of fibre-drawing processes.

Even when these assumptions are adopted, the axisymmetric free-boundary problem is formidable in general, and the other property of fibre draw-down that makes it ripe for mathematical simplification is the *slenderness* of the geometry. This can be characterized by the inverse aspect ratio ϵ, defined to be the ratio between a

† Present address: Laboratoire de Physique Statistique, École Normale Supérieure, 75231 Paris Cedex 05, France.

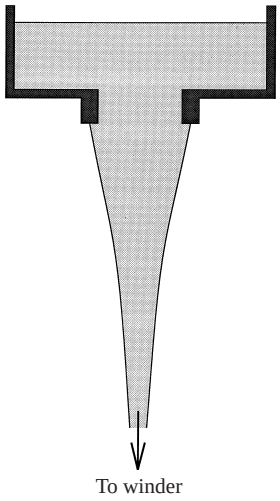

FIGURE 1. Schematic diagram of a fibre draw-down process.

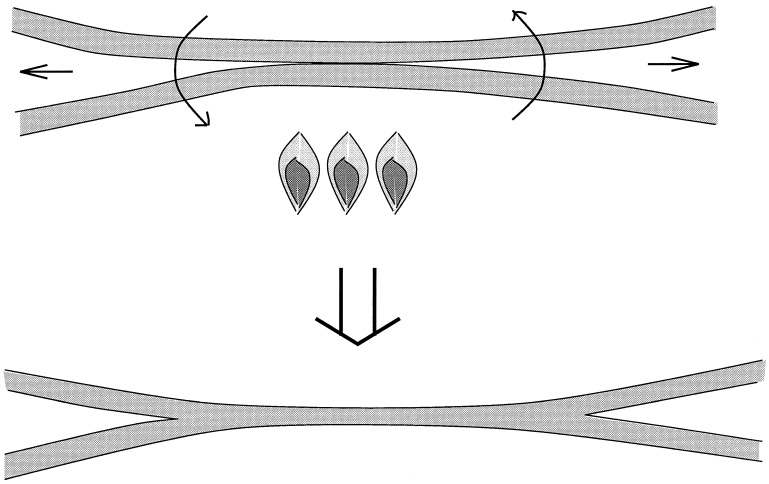

FIGURE 2. Schematic diagram of an optical fibre coupling process.

characteristic cross-sectional radius of the fibre and a typical length. When ϵ is small (it may be $O(10^{-3})$ for a draw-down process), greatly simplified models can be derived by expanding the governing (e.g. Navier–Stokes) equations and free-surface conditions in powers of ϵ – see for example Schultz & Davis (1982) or Ting & Keller (1990).

The original motivation for the current work is the manufacture of optical fibre couplers, shown schematically in figure 2. These are designed to allow signals carried by several different optical fibres to interact. Typically, they are produced by combining two or more strands of optical fibre which are then heated, twisted and/or stretched. Once the glass has melted, surface tension causes the fibres to coalesce, eventually forming a single axisymmetric fibre – a phenomenon known as *viscous sintering*. It is clear that in such a process the flow is inherently both *non-axisymmetric* and *unsteady*. However, it does have a small inverse aspect ratio, and this fact can still be used to obtain a simplified model from the three-dimensional Navier–Stokes equations and free-surface conditions.

This work follows the papers of Dewynne, Ockendon & Wilmott (1992) and Dewynne, Howell & Wilmott (1994), in which systematic asymptotic methods are used to derive equations governing the evolution of a slender, non-axisymmetric, Newtonian viscous fibre. In Dewynne *et al.* (1992) the analysis is restricted to viscous effects, while Dewynne *et al.* (1994) include the effects of inertia and gravity. In the latter paper, surface tension is also briefly considered, but only in the limit of large capillary number (in a sense to be defined later), in which it is shown to be negligible. In both papers, it is found that *each material cross-section of the fibre preserves its shape* as the fibre evolves, while undergoing a lateral translation, rotation and affine scaling in size. Indeed, this property is crucial for the solution procedure adopted for finding the twist of the fibre about its axis, namely transforming to a suitably scaled Lagrangian frame in which the geometry of the fibre is fixed.

It is clear that this shape-preserving property does not apply to the fibre-coupling process outlined above. In fact the change in shape of the cross-section, as it evolves towards a circle under surface tension, is crucial to the success of the process. Therefore in §§ 2–3 of this paper we extend the work of Dewynne *et al.* (1994) to flows where the capillary number is somewhat smaller (again, in a sense to be clarified later) and surface tension effects cannot be neglected. Several serious extra complications result, not least the fact that the shape of the cross-section is no longer known in advance: we have to obtain and solve a free-boundary problem for its evolution. This is particularly bothersome since we find that the shape of the cross-section enters the equations governing the axial stretching of the fibre. Moreover, since the option of transforming to a frame in which the fibre has fixed shape is no longer available, there are serious mathematical difficulties in finding the lateral translation and twist of the fibre, which we have thus far been unable to overcome.

However, in § 4 we show that the evolution of the shape of the cross-section decouples from these transverse motions, and is governed by a quasi-two-dimensional free-boundary problem similar to two-dimensional Stokes flow with a surface-tension-driven boundary. Thus we are able to exploit the complex-variable methods pioneered by Hopper (1990) and Richardson (1992) to find remarkably simple equations for the evolution of a large class of cross-section shapes; two examples are given in § 5. Further simplification of the method is obtained in § 6 by considering a fibre whose cross-section is nearly circular. This enables us to make some general statements about the final stages of the sintering process. Then in § 7 we present some sample numerical solutions which illustrate the various effects of surface tension, viscosity, inertia and gravity on the fibre evolution.

A Lagrangian coordinate transformation is employed in § 8 to elucidate the coupling between stretching and sintering of the fibre. The difficulty of the problem for lateral translation and rotation of the fibre is described further in § 9, and our final conclusions and a discussion of the implications of our numerical results are given in § 10. Details of certain manipulations are given in the Appendices.

2. The three-dimensional mathematical model

We consider the flow of a jet or fibre of viscous liquid like that shown schematically in figure 3. In setting up the problem we follow Dewynne *et al.* (1992, 1994), and use much the same notation. The fluid flow within the fibre is governed by the Navier–Stokes equations,

$$\rho(\boldsymbol{u}_t + (\boldsymbol{u}\cdot\nabla)\boldsymbol{u}) = -\nabla p + \mu\nabla^2\boldsymbol{u} + \rho g(\cos\beta, \sin\beta, 0), \tag{2.1a}$$

$$\nabla\cdot\boldsymbol{u} = 0, \tag{2.1b}$$

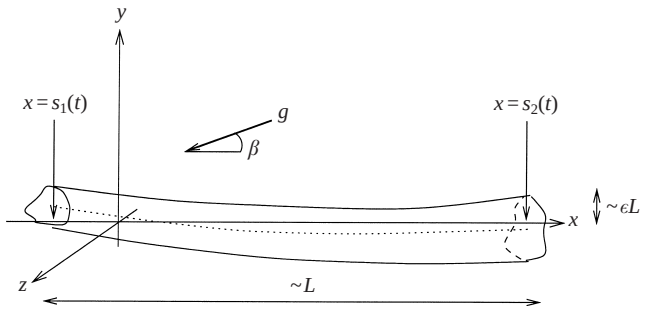

FIGURE 3. Definition sketch of a slender viscous fibre. The dotted line is the centre-line of the fibre, and the two ends are given by $x = s_1(t)$, $s_2(t)$.

where ρ and μ are the (constant) fluid density and viscosity, p and $\boldsymbol{u} = (u, v, w)$ are the pressure and fluid velocity, and g is the acceleration due to gravity (assumed to act at an angle β to the x-axis). If the free surface of the fibre is given by $G(x, y, z, t) = 0$, then the kinematic and stress boundary conditions may be written as

$$G_t + \boldsymbol{u} \cdot \nabla G = 0, \quad \boldsymbol{\sigma} \cdot \nabla G = -\gamma \kappa \nabla G, \quad \text{on } G = 0, \tag{2.2}$$

where γ is the coefficient of surface tension, κ is the mean curvature of the interface, and $\boldsymbol{\sigma} = \{\sigma_{ij}\}$ is the usual Newtonian stress tensor, given by

$$\sigma_{ij} = -p\delta_{ij} + \mu \left(\frac{\partial u_i}{\partial x_j} + \frac{\partial u_j}{\partial x_i} \right).$$

Initially the fibre shape and fluid velocity must be specified; the problem is then closed by prescribing the velocities of the two ends of the fibre, say

$$\boldsymbol{u} = \boldsymbol{u}_1^* \quad \text{at} \quad x = s_1(t), \quad \boldsymbol{u} = \boldsymbol{u}_2^* \quad \text{at} \quad x = s_2(t). \tag{2.3}$$

For example, we might imagine the two ends of the fibre to be attached to rigid planes perpendicular to the x-axis. In this case, the components v_i^* and w_i^* define a rigid-body motion corresponding to the lateral translation and twist applied at the ends, and $u_i^* = \dot{s}_i$.

The equations are non-dimensionalized in the obvious manner, assuming that the 'slenderness parameter' $\epsilon =$ (typical fibre radius)/(initial fibre length, L), is small. We set

$$(x, y, z) = L(\bar{x}, \epsilon\bar{y}, \epsilon\bar{z}), \quad t = \frac{L}{U}\bar{t},$$

$$\boldsymbol{u} = U(\bar{u}, \epsilon\bar{v}, \epsilon\bar{w}), \quad p = \frac{\mu U}{L}\bar{p}, \quad \kappa = \frac{1}{\epsilon L}\bar{\kappa},$$

where U is a typical pulling speed. Notice that by applying these scalings we also implicitly assume that the fibre is nearly straight, and choose the x-axis to lie approximately along its centre-line (as shown in figure 3). For a fibre where the curvature of the centre-line is not small, a fixed Cartesian coordinate system fails to capture the geometry, and curvilinear coordinates fixed in the moving fibre are preferable – see Howell (1994).

The important dimensionless parameters are the Reynolds, capillary and Stokes numbers, given by

$$Re = \frac{\rho U L}{\mu}, \quad Ca = \frac{\mu U}{\gamma}, \quad St = \frac{\rho L^2 g}{\mu U}.$$

In all the derivations to follow we assume that Re and St are both $O(1)$, so that viscous stresses, inertia and the axial component of gravity are all balanced. Notice, however, that a typical (dimensional) transverse displacement of the fibre due to gravity is

$$y \sim StL \sin\beta.$$

This scaling estimate can be obtained from a transverse force balance on the fibre as a whole: (tension) $\times$ (curvature) $\sim$ (gravity) where, if S is the area of the fibre cross-section, tension $\sim \mu SU/L$, curvature $\sim y/L^2$ and gravity $\sim \rho g S \sin\beta$. Since in this paper we assume that $y \sim \epsilon L$ we must either have small gravity ($St = O(\epsilon)$), in which case the axial component of gravity is negligible, or take the axis of the fibre to be almost vertical: $\beta = O(\epsilon)$.

For the capillary number, Dewynne *et al.* (1994) assume $Ca = O(\epsilon^{-3})$, so surface tension effects appear only at $O(\epsilon^2)$ and do not affect the leading-order problem. Here we consider the case where $Ca = O(\epsilon^{-1})$, and surface tension does enter the leading-order problem. We thus define a dimensionless surface tension coefficient,

$$\gamma^* = \frac{1}{\epsilon Ca} = O(1).$$

In summary, the scaling assumptions employed in this paper, namely

$$Re = O(1), \quad Ca = O(\epsilon^{-1}), \quad St = O(1), \quad \beta = O(\epsilon), \tag{2.4}$$

are chosen such that a leading-order balance is obtained between all the desired effects of viscosity, surface tension, inertia and gravity. Thus we obtain the most general leading-order model, which should be applicable to a wide variety of slender-jet flows. If in practice the scalings are different from (2.4) then we can deduce that one or more of these physical effects is negligible, and the correct leading-order equations can be obtained from our model by letting the appropriate parameters tend to zero or to infinity. For example, Howell (1994) gives the following approximate scalings for the optical fibre coupling process:

$$\epsilon \sim 10^{-3}, \quad Re \sim 10^{-7}, \quad Ca \sim 10^{3}, \quad St \sim 10^{-2}. \tag{2.5}$$

Hence for this process, there is a leading-order balance between viscosity and surface tension, but we can probably neglect inertia and gravity (i.e. set $Re = St = 0$).

Before moving on to the asymptotic analysis we quote the following transport theorems, introduced in Dewynne *et al.* (1992), which will be used in § 3 to simplify the equations:

$$\frac{\partial}{\partial t}\iint_S \phi \, \mathrm{d}y \, \mathrm{d}z = \iint_S \frac{\partial \phi}{\partial t} \, \mathrm{d}y \, \mathrm{d}z - \oint_{\partial S} \frac{G_t \phi \, \mathrm{d}s}{(G_y^2 + G_z^2)^{1/2}}, \tag{2.6a}$$

$$\frac{\partial}{\partial x}\iint_S \phi \, \mathrm{d}y \, \mathrm{d}z = \iint_S \frac{\partial \phi}{\partial x} \, \mathrm{d}y \, \mathrm{d}z - \oint_{\partial S} \frac{G_x \phi \, \mathrm{d}s}{(G_y^2 + G_z^2)^{1/2}}, \tag{2.6b}$$

$$\iint_S \frac{\partial \phi}{\partial y}\,\mathrm{d}y\,\mathrm{d}z = \oint_{\partial S} y\frac{(G_y\phi_y + G_z\phi_z)\,\mathrm{d}s}{(G_y^2+G_z^2)^{1/2}} - \iint_S y(\phi_{yy}+\phi_{zz})\,\mathrm{d}y\,\mathrm{d}z, \tag{2.6c}$$

$$\iint_S \frac{\partial \phi}{\partial z}\,\mathrm{d}y\,\mathrm{d}z = \oint_{\partial S} z\frac{(G_y\phi_y + G_z\phi_z)\,\mathrm{d}s}{(G_y^2+G_z^2)^{1/2}} - \iint_S z(\phi_{yy}+\phi_{zz})\,\mathrm{d}y\,\mathrm{d}z. \tag{2.6d}$$

Here S is any cross-sectional slice of the fibre in the (y,z)-plane and $\phi(x,y,z,t)$ is any twice continuously differentiable function.

3. Asymptotic analysis and one-dimensional model

The asymptotic analysis is very similar to that of Dewynne *et al.* (1994), and we omit unnecessary details. After non-dimensionalizing (2.1) and (2.2) acording to (1), we drop the overbars and expand each of the unknown functions (including the *a priori* unknown free boundary $G(x,y,z,t)$) as power series in ϵ^2 (e.g. $u \sim u_0+\epsilon^2 u_1+\epsilon^4 u_2+\cdots$). The leading-order Navier–Stokes equations, kinematic and stress boundary conditions are easily seen to be

$$u_{0_{yy}} + u_{0_{zz}} = 0, \tag{3.1a}$$

$$v_{0_{yy}} + v_{0_{zz}} = p_{0_y}, \tag{3.1b}$$

$$w_{0_{yy}} + w_{0_{zz}} = p_{0_z}, \tag{3.1c}$$

$$u_{0_x} + v_{0_y} + w_{0_z} = 0, \tag{3.1d}$$

$$G_{0_t} + u_0 G_{0_x} + v_0 G_{0_y} + w_0 G_{0_z} = 0 \quad \text{on } G_0 = 0, \tag{3.1e}$$

$$G_{0_y} u_{0_y} + G_{0_z} u_{0_z} = 0 \quad \text{on } G_0 = 0, \tag{3.1f}$$

$$G_{0_x} u_{0_y} + G_{0_y}(-p_0 + 2v_{0_y}) + G_{0_z}(v_{0_z} + w_{0_y}) = -\gamma^* \kappa_0 G_{0_y} \quad \text{on } G_0 = 0, \tag{3.1g}$$

$$G_{0_x} u_{0_z} + G_{0_y}(v_{0_z} + w_{0_y}) + G_{0_z}(-p_0 + 2w_{0_z}) = -\gamma^* \kappa_0 G_{0_z} \quad \text{on } G_0 = 0. \tag{3.1h}$$

The leading-order axial velocity u_0 satisfies a homogeneous Neumann problem (3.1a, f) which implies that it is independent of y and z, that is

$$u_0 = u_0(x,t). \tag{3.2}$$

Then, exactly as in Dewynne *et al.* (1994), by applying the transport theorems (2.6a, b) to the leading-order kinematic condition (3.1e), we obtain an equation representing global conservation of mass:

$$S_{0_t} + (u_0 S_0)_x = 0, \tag{3.3}$$

where S_0 is the leading-order cross-sectional area,

$$S_0 = \iint_{S_0} \mathrm{d}y\,\mathrm{d}z.$$

The cross-flow components of the stress boundary condition (3.1g, h) differ from those found by Dewynne *et al.* (1994) because of the surface tension terms on the right-hand sides. The general solution of the leading-order cross-flow problem with zero surface tension ((3.1b, c, d, g, h) with $\gamma^* \equiv 0$) was found by Dewynne *et al.* (1994) to be

$$P_{ZST} = -u_{0_x}, \tag{3.4a}$$

$$V_{ZST} = y_t^* + u_0 y_x^* - \tfrac{1}{2}u_{0_x}(y-y^*) + c(x,t)(z-z^*), \tag{3.4b}$$

$$W_{ZST} = z_t^* + u_0 z_x^* - \tfrac{1}{2}u_{0_x}(z-z^*) - c(x,t)(y-y^*), \tag{3.4c}$$

where $y^*(x,t)$, $z^*(x,t)$ and $c(x,t)$ are arbitrary functions. Physically, (y^*, z^*) represents the centre-line of the fibre, defined to be the line joining the centre of mass of each cross-section,

$$\boldsymbol{r}^*(x,t) = \begin{pmatrix} y^*(x,t) \\ z^*(x,t) \end{pmatrix} = \frac{1}{S_0} \iint_{S_0} \begin{pmatrix} y \\ z \end{pmatrix} \mathrm{d}y\,\mathrm{d}z,$$

while c corresponds to rotation in the (y,z)-plane:

$$c = \frac{1}{\mathscr{I}} \iint_{S_0} (z - z^*)v_0 - (y - y^*)w_0 \,\mathrm{d}y\,\mathrm{d}z, \tag{3.5}$$

where $\mathscr{I}$ is the moment of inertia of the cross-section,

$$\mathscr{I} = \iint_{S_0} (y - y^*)^2 + (z - z^*)^2 \,\mathrm{d}y\,\mathrm{d}z. \tag{3.6}$$

The subscripts ZST refer to the fact that (3.4) is a solution of the leading-order zero-surface-tension problem. As noted in Dewynne *et al.* (1994), from this form of the transverse velocity field, one can deduce that each material cross-section of the fibre maintains its shape, while undergoing lateral translation, twist and affine scaling.

For non-zero γ^*, (3.4) is no longer a solution (though we make use of it in §4) so this shape-preserving property is lost. We instead proceed by rewriting equations (3.1*b*, *c*) in the form

$$(-p_0 + 2v_{0_y})_y + (v_{0_z} + w_{0_y})_z = 0,$$

$$(v_{0_z} + w_{0_y})_y + (-p_0 + 2w_{0_z})_z = 0,$$

so that we may introduce an *Airy stress function* $\mathscr{A}$ for the cross-flow, such that

$$-p_0 + 2v_{0_y} = \mathscr{A}_{zz}, \tag{3.7a}$$

$$v_{0_z} + w_{0_y} = -\mathscr{A}_{yz}, \tag{3.7b}$$

$$-p_0 + 2w_{0_z} = \mathscr{A}_{yy}. \tag{3.7c}$$

The problem satisfied by $\mathscr{A}$ is

$$\hat{\nabla}^4 \mathscr{A} = 0 \quad \text{in } S_0; \quad \mathscr{A} = 0, \frac{\partial \mathscr{A}}{\partial \hat{n}} = -\gamma^* \quad \text{on } \partial S_0, \tag{3.8}$$

where $\hat{\nabla} = (0, \partial_y, \partial_z)$ is the two-dimensional gradient operator, and $\hat{\boldsymbol{n}} = \hat{\nabla} G_0 / |\hat{\nabla} G_0|$ is the two-dimensional normal to the cross-section.† If G_0 is known then $\mathscr{A}$ is given uniquely by (3.8); in particular, $\mathscr{A} \equiv 0$ if and only if $\gamma^* = 0$. However in general the boundary-value problem for $\mathscr{A}$ must be solved anew at each time-step as the cross-section evolves according to the kinematic condition (3.1*e*).

Once $\mathscr{A}$ is known the leading-order pressure and transverse velocity gradients are found using (3.7):

$$p_0 = -\tfrac{1}{2}(\mathscr{A}_{yy} + \mathscr{A}_{zz}) - u_{0_x}, \tag{3.9a}$$

† The problem (3.8) has been simplified in the usual way using the fact that $\mathscr{A}$ is only defined up to a linear function of y and z. By substituting (3.7) into the boundary conditions (3.1*g*, *h*) one can readily deduce that $\hat{\nabla}\mathscr{A} + \gamma^* \hat{\boldsymbol{n}}$ is constant on the boundary. However, this constant vector may without loss of generality be set to zero, resulting in $\partial \mathscr{A}/\partial \hat{n} = -\gamma^*$, $\mathscr{A}$ = constant. Finally, this constant may also be chosen to be zero, resulting in the standard boundary conditions (3.8).

$$v_{0_y} = \tfrac{1}{4}(\mathscr{A}_{zz} - \mathscr{A}_{yy}) - \tfrac{1}{2}u_{0_x}, \tag{3.9b}$$

$$w_{0_z} = \tfrac{1}{4}(\mathscr{A}_{yy} - \mathscr{A}_{zz}) - \tfrac{1}{2}u_{0_x}. \tag{3.9c}$$

However, these do not determine v_0 and w_0 uniquely, for the zero-surface-tension solution (3.4) serves as an eigenfunction of the homogeneous problem ((3.9) with $\mathscr{A} \equiv 0$). The lack of uniqueness in the leading-order cross-flow corresponds to the property of two-dimensional Stokes flow with surface tension that an arbitrary rigid-body motion can be added to the flow. To determine v_0 and w_0 uniquely we must proceed to higher order and find three equations governing the lateral motion and rotation of the cross-section (i.e. the three arbitrary functions y^*, z^* and c).

The problem for the first-order axial velocity is simply the x-component of the Navier–Stokes equation and stress boundary condition at order ϵ^2, namely†

$$u_{1_{yy}} + u_{1_{zz}} = Re(u_{0_t} + u_0 u_{0_x}) + p_{0_x} - u_{0_{xx}} - St\cos\beta \quad \text{in } S_0; \tag{3.10a}$$

$$u_{1_y} G_{0_y} + u_{1_z} G_{0_z} = G_{0_x}(p_0 - 2u_{0_x} - \gamma^* \kappa_0) - G_{0_y} v_{0_x} - G_{0_z} w_{0_x} \quad \text{on } \partial S_0. \tag{3.10b}$$

Now we apply the solvability condition, which for this inhomogeneous Neumann problem is just the identity

$$\int\!\!\int_{S_0} \hat{\nabla}^2 u_1 \, \mathrm{d}y \, \mathrm{d}z = \oint_{\partial S_0} \frac{\partial u_1}{\partial \hat{n}} \, \mathrm{d}s. \tag{3.11}$$

The evaluation of the integrals involves some tedious manipulations, the details of which can be found in Appendix A. Denoting by Γ_0 the leading-order circumference of the cross-section,

$$\Gamma_0 = \oint_{\partial S_0} \mathrm{d}s,$$

the resulting equation is

$$(3S_0 u_{0_x})_x = ReS_0(u_{0_t} + u_0 u_{0_x}) - S_0 St\cos\beta - \tfrac{1}{2}\gamma^* \Gamma_{0_x}, \tag{3.12}$$

which is an axial stress balance for the fibre (identical to equation (16) of Dewynne *et al.* (1994) when $\gamma^* \equiv 0$). Once this solvability condition has been satisfied, assuming G_0 is known (3.10) determines u_1 up to an arbitrary function of x and t.

To recap, thus far we have two equations (3.3), (3.12) for the leading-order axial velocity u_0, cross-sectional area S_0 and circumference Γ_0 of the fibre. In the zero-surface-tension limit $\gamma^* \to 0$, we retrieve the closed system for u_0 and S_0 found by Dewynne *et al.* (1994). Alternatively, if the cross-section is assumed to be circular, then we have $\Gamma_0 = 2\sqrt{\pi S_0}$ and so again a closed problem for u_0 and S_0 is obtained (indeed this model has been used previously to model axisymmetric fibres, for example by Eggers & Dupont (1994)). However, in general to make further progress with (3.3) and (3.12) we need to know how Γ_0 and S_0 are related, that is we must determine how the shape of the cross-section evolves.

Before attempting to do so, we derive equations for the lateral translation and twist of the fibre from solvability conditions for the first-order cross-flow. The equations

† Note that in this and other similar equations to come, we do not assume $G_1 = 0$; it would be inconsistent to do so since according to the $O(\epsilon^2)$ term in (2.2) G_1 evolves subject to the first-order velocity components. It simply transpires that the coefficients of terms involving G_1 are identically zero.

and boundary conditions at $O(\epsilon^2)$ are

$$u_{1_x} + v_{1_y} + w_{1_z} = 0, \tag{3.13a}$$

$$Re(v_{0_t} + u_0 v_{0_x} + v_0 v_{0_y} + w_0 v_{0_z}) = St \sin\beta/\epsilon - p_{1_y} + v_{0_{xx}} + v_{1_{yy}} + v_{1_{zz}}, \tag{3.13b}$$

$$Re(w_{0_t} + u_0 w_{0_x} + v_0 w_{0_y} + w_0 w_{0_z}) = -p_{1_z} + w_{0_{xx}} + w_{1_{yy}} + w_{1_{zz}}, \tag{3.13c}$$

$$G_{0_x}(u_{1_y} + v_{0_x}) + G_{0_y}(-p_1 + 2v_{1_y}) + G_{0_z}(v_{1_z} + w_{1_y}) = -\gamma^* \kappa_1 G_{0_y} \quad \text{on} \partial S_0, \tag{3.13d}$$

$$G_{0_x}(u_{1_z} + w_{0_x}) + G_{0_y}(v_{1_z} + w_{1_y}) + G_{0_z}(-p_1 + 2w_{1_z}) = -\gamma^* \kappa_1 G_{0_z} \quad \text{on } \partial S_0, \tag{3.13e}$$

where κ_1 is the first-order perturbation to the mean curvature of the free surface. Integration of (3.13*b*) and (3.13*c*) over the cross-section with the boundary conditions (3.13*d*) and (3.13*e*) gives the lateral force balance. One can use the equations and boundary conditions satisfied by u_1, v_0, w_0 and p_0 to eliminate them from the integrated equations, and thus write the surface tension terms in a form which depends only on the shape of the cross-section. Further details of the required calculation are given in Appendix B; their result is the following equation for the motion of the centre-line $\boldsymbol{r}^*(x,t)$:

$$\begin{aligned}(Reu_0^2 - 3u_{0_x})\boldsymbol{r}^*_{xx} + 2Reu_0\boldsymbol{r}^*_{xt} + Re\boldsymbol{r}^*_{tt} - (St\sin\beta/\epsilon)\boldsymbol{j} + St\cos\beta\boldsymbol{r}^*_x \\ = -\frac{\gamma^*}{S_0}\left\{\frac{\Gamma_0}{2}\boldsymbol{r}^*_{xx} + \Gamma_{0_x}\boldsymbol{r}^*_x + \frac{1}{2}\frac{\partial^2}{\partial x^2}\oint_{\partial S_0}(\boldsymbol{r}-\boldsymbol{r}^*)\mathrm{d}s \right. \\ \left. + \frac{\partial}{\partial x}\oint_{\partial S_0}\frac{(\boldsymbol{r}-\boldsymbol{r}^*)\kappa_0 G_{0_x}\mathrm{d}s}{\sqrt{G_{0_y}^2 + G_{0_z}^2}} + \oint_{\partial S_0}\kappa_1\hat{\boldsymbol{n}}\mathrm{d}s\right\},\end{aligned} \tag{3.14}$$

where $\boldsymbol{j}$ is (as usual) the unit vector in the y-direction. This equation should be compared with its zero-surface-tension counterpart, (22) in Dewynne *et al.* (1994), and the details of the derivation are similar. Note from the inhomogeneous terms on the right-hand side that if ∂S_0 lacks symmetry then surface tension can impart lateral momentum to the cross-section, that is $\boldsymbol{r}^* \equiv \boldsymbol{0}$ may not be a solution.

An equation for the twist of the fibre about its axis can also be obtained by taking moments of (3.13*b*) and (3.13*c*), before integrating over the cross-section S_0. Further details are given in Appendix C, where the following equation is obtained:

$$\begin{aligned}\frac{\partial}{\partial x}\iint_{S_0}\{y(w_{0_x} + u_{1_z}) - z(v_{0_x} + u_{1_y})\}\,\mathrm{d}y\,\mathrm{d}z = ReS_0(L_{0_t} + u_0 L_{0_x}) \\ - \frac{S_0 St z^*\sin\beta}{\epsilon} + \gamma^*\oint_{\partial S_0}\frac{\kappa_1(yG_{0_z} - zG_{0_y})\mathrm{d}s}{\sqrt{G_{0_y}^2 + G_{0_z}^2}},\end{aligned} \tag{3.15}$$

where L_0 is the average (leading-order) angular momentum of the cross-section,

$$L_0 = \frac{1}{S_0}\iint_{S_0}(yw_0 - zv_0)\,\mathrm{d}y\,\mathrm{d}z.$$

In general the problem must be solved as follows. Given the shape of the cross-section at some time, the axial velocity u_0 may be found from (3.12). Then (3.8) must be solved for $\mathscr{A}$, in terms of which v_0 and w_0 are determined up to an arbitrary rigid-body motion. The rigid-body translation is given by (3.14) and the rotation by (3.15), which also requires the solution of the Neumann problem (3.10) for u_1. Once

u_0, v_0 and w_0 have been found, the evolution of the cross-section is given by the kinematic boundary condition (3.1*e*).

Clearly, a complete solution of the leading-order problem is a formidable task in general, and one which we shall not attempt. For example, the equation (3.15) for the twist of the fibre involves the solution u_1 of a Neumann problem (3.10) which must be evaluated anew at each time-step as the cross-section evolves. Dewynne *et al.* (1994) showed that when $\gamma^* = 0$ the problem can be greatly simplified by transforming to suitably defined Lagrangian variables, in which the geometry of the fibre is fixed, so that the Neumann problem (3.10) need only be solved once. The success of this approach relies on the shape-preserving property of zero-surface-tension fibres noted earlier. With $\gamma^* \neq 0$ this property is lost, so the twisting problem does not appear to be significantly simplified by a Lagrangian approach.

An even greater hurdle is the presence of the first-order free-surface curvature κ_1 in equations (3.14), (3.15); we discuss the implications of this further in § 9. Therefore in this paper we do not attempt to solve for the lateral motion and twist of the fibre. Nonetheless significant progress can still be made, since in the following Section we show that the evolution of the shape of the cross-section can be determined independently of the translation and twist.

4. The use of complex-variable methods to determine the evolution of the shape of the cross-section

Throughout this section we drop the suffices on the leading-order variables, so that G_0, κ_0, S_0, p_0, $u_0, \ldots$ are replaced by G, κ, S, p, $u, \ldots$. Consider the problem for the leading-order cross-flow, (3.1*b–d*), with boundary conditions (3.1*e*, *g*, *h*). We first subtract off the zero-surface-tension eigensolution (3.4), setting

$$p = P_{ZST} + \tilde{p}, \quad v = V_{ZST} + \tilde{v}, \quad w = W_{ZST} + \tilde{w}.$$

As a result of this definition, $\tilde{v}$ and $\tilde{w}$ satisfy

$$\iint_S \begin{pmatrix} \tilde{v} \\ \tilde{w} \end{pmatrix} \mathrm{d}y\, \mathrm{d}z = 0,$$

and the function $c(x,t)$ is chosen to account for the net rotation of the cross-section, so that

$$\iint_S ((y - y^*)\tilde{w} - (z - z^*)\tilde{v})\, \mathrm{d}y\, \mathrm{d}z = 0. \tag{4.1}$$

Hence with respect to the tilded variables, the cross-section has no linear or angular momentum.

In terms of these new variables the cross-flow problem becomes

$$\tilde{v}_y + \tilde{w}_z = 0, \tag{4.2a}$$

$$\tilde{v}_{yy} + \tilde{v}_{zz} = \tilde{p}_y, \tag{4.2b}$$

$$\tilde{w}_{yy} + \tilde{w}_{zz} = \tilde{p}_z, \tag{4.2c}$$

$$G_y(-\tilde{p} + 2\tilde{v}_y) + G_z(\tilde{v}_z + \tilde{w}_y) = -\gamma^* \kappa G_y \quad \text{on } G = 0, \tag{4.2d}$$

$$G_y(\tilde{v}_z + \tilde{w}_y) + G_z(-\tilde{p} + 2\tilde{w}_z) = -\gamma^* \kappa G_z \quad \text{on } G = 0, \tag{4.2e}$$

which is the same as the problem of two-dimensional Stokes flow with a surface

tension driven boundary, though with a modified kinematic condition:

$$G_t + \tilde{v}G_y + \tilde{w}G_z = -uG_x - (y_t^* + uy_x^*)G_y - (z_t^* + uz_x^*)G_z$$
$$+\tfrac{1}{2}u_x((y-y^*)G_y + (z-z^*)G_z) + c((y-y^*)G_z - (z-z^*)G_y) \quad \text{on } G = 0. \quad (4.3)$$

In the classical two-dimensional Stokes flow problem, the right-hand side of (4.3) is zero. The extra terms in our problem arise from (i) flow between adjoining cross-sections (the terms involving the axial velocity u) and (ii) the translation and rotation of the cross-section (represented by y^*, z^* and c). If, in (4.3), the axial velocity u is set to zero, the well-known invariance of the two-dimensional Stokes flow problem and (stress) boundary conditions with respect to any rigid-body motion can be used to eliminate y^*, z^* and c so that the right-hand side of (4.3) is identically zero and the classical two-dimensional Stokes flow problem is recovered. Hopper (1990) and Richardson (1992) showed that in many cases exact solutions to this problem may be found in terms of a time-dependent univalent map $f(\zeta, t)$ from the unit disc $\{|\zeta| \leqslant 1\}$ onto the cross-section, and Richardson (1992) gave a general procedure for constructing such solutions when the mapping function is rational. In this Section we closely follow the approach of that paper, showing how the ideas can be adapted to our problem.

We write the velocity components $\tilde{v}$, $\tilde{w}$ in terms of a streamfunction ψ:

$$\tilde{v} = \psi_z, \quad \tilde{w} = -\psi_y.$$

As a consequence of (4.2*b*, *c*), ψ must satisfy the biharmonic equation and so, using the Goursat representation of biharmonic functions, may be expressed in the form

$$\psi = -\mathrm{Im}\left\{\bar{\mathscr{Z}}\phi(\mathscr{Z}) + \chi(\mathscr{Z})\right\},$$

where ϕ and χ are analytic functions of the complex variable $\mathscr{Z} = y + \mathrm{i}z$ for $(y, z) \in S$. These 'Goursat functions' provide a complete description of the flow, and all physical quantities of interest may be written in terms of them; for instance the velocity components and pressure are given by

$$\tilde{v} + \mathrm{i}\tilde{w} = \phi(\mathscr{Z}) - \mathscr{Z}\overline{\phi'(\mathscr{Z})} - \overline{\chi'(\mathscr{Z})},$$

$$\tilde{p} = -4\mathrm{Re}\left\{\phi'(\mathscr{Z})\right\}.$$

The stress boundary conditions (4.2*d*, *e*) are easily seen to combine to give the single complex boundary condition

$$\phi(\mathscr{Z}) + \mathscr{Z}\overline{\phi'(\mathscr{Z})} + \overline{\chi'(\mathscr{Z})} = \frac{\mathrm{i}\gamma^*}{2}\frac{\mathrm{d}\mathscr{Z}}{\mathrm{d}s}, \quad (4.4)$$

where s is arclength around the cross-section (measured in the anticlockwise sense in the (y, z)-plane).

Assuming that the boundary is an analytic curve, the cross-section $S(x, t)$ may be described as the image of the unit disc $\{|\zeta| \leqslant 1\}$ under a univalent map $f : \zeta \mapsto \mathscr{Z}$ which depends on distance x along the fibre, and on t. For simplicity we first eliminate rotation and translation of S and write

$$\mathscr{Z} = \mathscr{Z}^*(x, t) + f(\zeta; x, t)\mathrm{e}^{-\mathrm{i}\alpha(x,t)},$$

where $\mathscr{Z}^* = y^* + \mathrm{i}z^*$ is the centre-line of the fibre and $\alpha(x, t)$, which represents the rotation, is related to the function $c(x, t)$ by

$$\alpha_t + u\alpha_x = c. \quad (4.5)$$

Henceforth the dependence of the various functions on x and t will be implicit; we shall denote $f_\zeta(\zeta, x, t)$ by $f'(\zeta)$, and so on.

Following Richardson (1992) we observe that $\mathrm{d}\mathscr{Z}/\mathrm{d}s$ in (4.4) has the representation

$$\frac{\mathrm{d}\mathscr{Z}}{\mathrm{d}s} = \mathrm{i}\zeta \frac{f'(\zeta)}{\left(\bar{f}'(1/\zeta)f'(\zeta)\right)^{1/2}} \quad \text{on } |\zeta| = 1,$$

in terms of ζ. One then splits up the square-root term in the denominator of the right-hand side as

$$\left(f'(\zeta)\bar{f}'(1/\zeta)\right)^{-1/2} = \mathscr{F}_+(\zeta) - \mathscr{F}_-(\zeta), \tag{4.6}$$

where $\mathscr{F}_+(\zeta)$ is analytic inside the unit circle, and $\mathscr{F}_-(\zeta)$ is analytic outside the unit circle, and decays to zero at infinity (this latter condition ensures the uniqueness of the decomposition (4.6); explicit formulae for the functions $\mathscr{F}_+$, $\mathscr{F}_-$ are given in Richardson 1992).

Defining the complex functions†

$$\Phi(\zeta) = \phi(f(\zeta)), \quad \mathscr{X}(\zeta) = \chi(f(\zeta)),$$

the stress boundary condition (4.4) holding on ∂S in the $\mathscr{Z}$-plane can then be transferred to the unit circle in the ζ-plane and written in the form (analogous to equation (2.18) of Richardson 1992)

$$\Phi(\zeta) + \frac{\gamma^*}{2}\mathscr{F}_+(\zeta)\zeta f'(\zeta) = -(\mathscr{Z}^* + f(\zeta)\mathrm{e}^{-\mathrm{i}\alpha})\frac{\bar{\Phi}'(1/\zeta)}{\bar{f}'(1/\zeta)} - \mathrm{e}^{\mathrm{i}\alpha}\frac{\bar{\mathscr{X}}'(1/\zeta)}{\bar{f}'(1/\zeta)} + \frac{\gamma^*}{2}\mathscr{F}_-(\zeta)\zeta f'(\zeta). \tag{4.7}$$

This equation holds not only on $|\zeta| = 1$, but everywhere these functions are defined in the ζ-plane, by analytic continuation. The kinematic boundary condition (4.3) may also be translated into complex-variable notation. The result (which is analogous to the second equation on p. 199 in Richardson 1992) is

$$\mathrm{Re}\left\{\frac{1}{\zeta f'(\zeta)}\left[2\Phi(\zeta)\mathrm{e}^{\mathrm{i}\alpha} - (f_t(\zeta) + uf_x(\zeta) + \tfrac{1}{2}u_x f(\zeta))\right] + \gamma^*\mathscr{F}_+(\zeta)\right\} = \frac{\gamma^*}{2}\mathscr{F}_+(0), \tag{4.8}$$

holding on $|\zeta| = 1$.

In the two-dimensional problem of Richardson (1992), symmetry of the fluid domain about the x-axis (our y-axis) is assumed, which enables (4.8) to be simplified. The equivalent assumption in our analysis is that the cross-section be symmetric about some axis which rotates with the angular speed c of the fibre. Insisting that this symmetry is preserved ensures that the angular momentum of the cross-section in the rotating frame is zero (as required by (4.1)). Without loss of generality then we may take $f(\zeta)$ and $\Phi(\zeta)\mathrm{e}^{\mathrm{i}\alpha}$ to be real whenever ζ is real. We also assume that the centre-line coordinate $\mathscr{Z}^*$ is everywhere inside the cross-section S, so that as in Richardson (1992) we may take $f(0; x, t) = 0$ and $\Phi(0; x, t) = 0$ for all x and t. With these assumptions the argument presented in Richardson (1992) follows through here, and we deduce that the function in curly brackets on the left-hand side of (4.8) is a real constant equal to the one on the right-hand side. That is, we may simply remove the 'Re' from the left-hand side and thus obtain a second globally holding equation (analogous to (2.19) in Richardson 1992).

† NB: There is a slight difference between our notation and that of Richardson (1992); he defines a function $X(\zeta) = \chi'(f(\zeta))$. This is related to our function $\mathscr{X}(\zeta)$ by $X(\zeta) = \mathscr{X}'(\zeta)/f'(\zeta)$.

We can substitute for $\Phi(\zeta)$ from this equation in (4.7) (if we first replace ζ by $1/\zeta$ in (4.7) and take the complex conjugate). This yields a functional equation for $\mathscr{X}'(\zeta)$ in terms of quantities which depend only on the mapping function f and the axial velocity u. When doing this it is helpful to define the differential operators $\mathrm{D} := \partial_t + u\partial_x + u_x$, and $\mathrm{E} := \partial_t + u\partial_x + u_x/2$, where the u_x terms are understood only to multiply whatever function the operator is acting on (so for example $\mathrm{D}[\cdot] = (\cdot)_t + (u\cdot)_x$). The result is

$$\mathrm{D}[f'(\zeta)\bar{f}(1/\zeta)] + \mathrm{e}^{-\mathrm{i}\alpha}\bar{\mathscr{Z}}^* \frac{\partial}{\partial\zeta}\left[\mathrm{E}[f(\zeta)] + \frac{\gamma^*}{2}\zeta f'(\zeta)\mathscr{G}(\zeta)\right] + 2\mathrm{e}^{-\mathrm{i}\alpha}\mathscr{X}'(\zeta) = \frac{\gamma^*}{2}\frac{\partial}{\partial\zeta}[\zeta f'(\zeta)\bar{f}(1/\zeta)\mathscr{G}(\zeta)], \quad (4.9)$$

where $\mathscr{G}(\zeta) := 2\mathscr{F}_+(\zeta) - \mathscr{F}_+(0)$. The explicit formula for $\mathscr{G}$ follows from the expression for $\mathscr{F}_+$ given in Richardson (1992), and is

$$\mathscr{G}(\zeta) = \frac{1}{2\pi\mathrm{i}}\oint_{|\tau|=1} \frac{1}{|f'(\tau)|}\left(\frac{\tau+\zeta}{\tau-\zeta}\right)\frac{\mathrm{d}\tau}{\tau}, \quad |\zeta| \leqslant 1, \quad (4.10)$$

the analytic continuation of this function being understood if we wish to extend (4.9) outside the unit disc.

The solution procedure is to propose a suitable rational map f whose coefficients depend on x and t, and then to equate the singularities within the unit disc on either side of equation (4.9), using the fact that $\mathscr{X}(\zeta)$ must be analytic there. This procedure yields a system of partial differential equations for the coefficients of f, which depend also on the axial velocity $u(x,t)$. The system of PDEs is closed by the axial stress balance (3.12), and the solution is completed by solving the coupled system. Once the coefficients of the map have been found, the evolution of the cross-section is determined.

4.1. *Conservation laws for viscous fibres*

It is interesting to note that the complex-variable formulation of §4 allows a quick alternative derivation of some of the results of Dewynne *et al.* (1992, 1994). There, surface tension effects are assumed to be negligible (and Dewynne *et al.* 1992 also neglect inertia and gravity). Consider the quantities $C_k(x,t)$ defined (for integers $k \geqslant 0$) by the integrals over the cross-section,

$$C_k(x,t) := \int\!\!\int_S \zeta(z)^k \,\mathrm{d}y\,\mathrm{d}z. \quad (4.11)$$

Applying Green's theorem in complex form (see Nehari 1975 for example) we can express the C_k as integrals around the boundary ∂S, and hence as integrals around the unit circle in the ζ-plane:

$$C_k = \frac{1}{2\mathrm{i}}\oint_{\partial S} \zeta^k \bar{z}\mathrm{d}z = \frac{1}{2\mathrm{i}}\oint_{|\zeta|=1} \zeta^k f'(\zeta)\bar{f}(1/\zeta)\mathrm{d}\zeta.$$

Then, multiplying equation (4.9) (with $\gamma^* = 0$) through by ζ^k and integrating around the unit circle yields the infinite system of conservation laws,

$$\mathrm{D}[C_k] = 0 \quad (k \geqslant 0), \quad (4.12)$$

where D is the operator defined earlier. Thus the quantities $C_k(x,t)$ are all conserved with respect to the operator D. This is analogous to the usual two-dimensional result that zero-surface-tension Stokes flow is completely trivial in the absence of driving

singularities (see Cummings, Howison & King 1997 for the two-dimensional case of this analysis, with a driving singularity). The $k = 0$ equation is exactly the mass conservation result (3.3).

In terms of the usual convective derivative, (4.12) reads

$$\frac{1}{C_k}\frac{\mathscr{D}C_k}{\mathscr{D}t} = -u_x, \tag{4.13}$$

which shows that for each material cross-section of the fibre, all of the quantities C_k evolve at the same rate: the local rate of extension. This is equivalent to the shape-preserving property of zero-surface-tension fibres noted by Dewynne *et al.* (1992, 1994).

A similar system of equations for the C_k may be written down for the non-zero-surface-tension case, and is

$$\mathrm{D}[C_k] = \begin{cases} 0 & (k = 0), \\ -\dfrac{k\gamma^*}{2}\displaystyle\sum_{r=0}^{\infty}\frac{\mathscr{G}^{(r)}(0)}{r!}C_{k+r} & (k \geqslant 1). \end{cases} \tag{4.14}$$

The above result holds when all physical effects considered in this paper are included; however the notation employed (suppressing the x and t dependence) makes it look deceptively simple. The function $\mathscr{G}$ is defined in (4.10) in terms of an integral involving the univalent map, which will in general be difficult to evaluate explicitly. Hence even if we assume a polynomial form for f (in which case only a finite number of the C_k are non-zero) it is very difficult to make analytical progress with the resulting system.

5. Two families of explicit solutions

We now consider specific examples of mapping functions $f(\zeta; x, t)$. The choices made (a polynomial and a rational mapping function) are sufficiently simple to allow analytical progress, and yield two classes of solutions. To determine fully the evolution, the resulting systems of PDEs for the coefficients must be solved numerically. For reasons of space we present sample numerical results only for the first class of solutions (§ 7); however it is clear that there is considerable potential for (and in fact the authors have performed) many more simulations.

Example 1

We begin with the family of simple polynomial maps (this same family was considered by Howison & Richardson (1995) for the two-dimensional Stokes flow problem with suction/injection)

$$f(\zeta; x, t) = a(x, t)\left(\zeta - \frac{b(x, t)}{n}\zeta^n\right), \tag{5.1}$$

for integers $n > 2$. We assume $a(x, t) > 0$ without loss of generality; the map is then univalent provided $|b(x, t)| < 1$. When $b = 1$ the map loses univalency via the formation of $(n-1)$ cusps in the boundary of the cross-section.

The only singularity of (4.9) is at $\zeta = 0$, and we can evaluate the behaviour there explicitly. On the right-hand side we find

$$\frac{\gamma^*}{2}\frac{\partial}{\partial\zeta}[\zeta f'(\zeta)\bar{f}(1/\zeta)\mathscr{G}(\zeta)] = \frac{\gamma^*(n-1)ab}{n\pi\zeta^n}K(b) + O(1) \quad \text{near } \zeta = 0,$$

where $K(\cdot)$ denotes the complete elliptic integral of the first kind (see for example Byrd & Friedman 1971 or Gradshteyn & Ryzhik 1980), while on the left-hand side

$$\mathrm{D}[f'(\zeta)\bar{f}(1/\zeta)] = -\frac{\mathrm{D}[a^2 b]}{n\zeta^n} + \mathrm{D}\left[a^2(1+b^2/n)\right]\frac{1}{\zeta} + O(1) \quad \text{near } \zeta = 0.$$

Hence matching these singularities we find two PDEs governing the evolution of $a(x,t)$, $b(x,t)$:

$$\mathrm{D}[\pi a^2(1+b^2/n)] \equiv \mathrm{D}[S] = 0, \tag{5.2}$$

$$\mathrm{D}[a^2 b] = -\frac{\gamma^*(n-1)ab}{\pi}K(b). \tag{5.3}$$

(Note that this system is a special case of (4.14).) The dependence on $u(x,t)$ is through the differential operator D. The third equation we need is the axial stress balance (3.12), for which we need to compute the circumference of the cross-section, $\Gamma(x,t)$. We have

$$\begin{aligned}\Gamma &= \oint_{\partial S} \mathrm{d}s = \oint_{\partial S} |\mathrm{d}\mathscr{Z}| = \int_0^{2\pi} |f'(\mathrm{e}^{\mathrm{i}\theta})|\mathrm{d}\theta \\ &= 4a(2E(b) - (1-b^2)K(b)),\end{aligned} \tag{5.4}$$

where $E(\cdot)$ is the complete elliptic integral of the second kind, and using identities given in Gradshteyn & Ryzhik 1980 we find

$$\frac{\partial \Gamma}{\partial x} = \frac{4(a^2 b)_x}{ab}E(b) - \frac{4(1-b^2)(ab)_x}{b}K(b).$$

Hence the axial stress balance (3.12) reduces to

$$\begin{aligned}(3Su_x)_x = ReS(u_t + uu_x) - StS\cos\beta - \frac{2\gamma^*(a^2 b)_x}{ab}E(b) \\ +2\gamma^*(1/b - b)(ab)_x K(b).\end{aligned} \tag{5.5}$$

Equations (5.2), (5.3), (5.5), subject to boundary conditions on $u(x,t)$ and initial conditions on $a(x,t)$, $b(x,t)$, together determine the cross-sectional evolution. This represents a considerable simplification of the full three-dimensional, and even the quasi-one-dimensional problems, but any further progress necessitates numerical work; this is carried out in § 7.

Example 2

The other family of mapping functions we consider consists of simple rational maps,

$$f(\zeta; x, t) = \frac{na(x,t)b(x,t)\zeta}{1 - b(x,t)^n\zeta^n}, \tag{5.6}$$

where $n \geqslant 2$ is an integer, $0 < b < b_c = (n-1)^{-1/n}$ to ensure univalency of the map, and $a > 0$ without loss of generality. The limit $b \to 0$, $a \to \infty$ describes a circular cross-section, and for $n \geqslant 3$ the limit $b \to b_c$ describes cross-sections with n inward-pointing cusps (rather similar to the $(n+1)$-degree polynomial solution); however for $n = 2$, $b_c = 1$ and the limit $b \to 1$ describes a cross-section consisting of two equal circles touching at a single point – such a configuration is of particular interest in the manufacture of optical fibre couplers.

Equation (4.9) now has singularities at points $\zeta = 0$ and $\zeta = b$ within the unit disc, which must be matched. Matching at $\zeta = 0$ simply gives the mass conservation result,

$$\mathrm{D}[S] = 0, \quad \text{where } S = \frac{\pi n^2 a^2 b^2 (1 + (n-1)b^{2n})}{(1 - b^{2n})^2} \tag{5.7}$$

(a straightforward integration verifies the latter equality), while matching at $\zeta = b$ yields a second PDE,

$$\frac{\partial b}{\partial t} + u\frac{\partial b}{\partial x} = -\frac{\gamma^* b(1 - b^{2n})}{n\pi ab} K\left((n-1)b^n\right). \tag{5.8}$$

In deriving this simple form for the right-hand side use was made of the formula (see Byrd & Friedman 1971 for example)

$$\frac{1}{1 + (n-1)b^n} K\left(\frac{2b^{n/2}(n-1)^{1/2}}{1 + (n-1)b^n}\right) = K((n-1)b^n).$$

The problem is again closed by the axial stress balance (3.12), with the circumference Γ given by (5.4) as

$$\Gamma = \frac{4n(n-1)ab}{1 + (n-1)b^n} \left\{ \frac{n(1 + (n-1)b^{2n})}{(n-1)(1 - b^n)^2} \Pi\left(\frac{-4b^n}{(1 - b^n)^2}, k\right) - K(k) \right\},$$

where $k = 2b^{n/2}(n-1)^{1/2}/(1 + (n-1)b^n)$ and $\Pi(\cdot, \cdot)$ denotes the complete elliptic integral of the third kind (see Byrd & Friedman 1971 or Gradshteyn & Ryzhik 1980 for a definition).

Again, equations (5.7), (5.8) and (3.12) (with Γ as above), subject to boundary conditions on $u(x,t)$ and initial conditions on $a(x,t)$, $b(x,t)$, determine the cross-sectional evolution.

6. Linear theory for a nearly circular cross-section

One problem with the complex-variable formulation of § 4 is that, without posing a particular form of the map f, it is difficult to infer general properties of the solution from equation (4.9). Some further intuition is gained by considering a fibre whose cross-section is nearly circular (this will eventually be true of any fibre after a sufficient time). We therefore consider maps of the form

$$f = a(x,t)\left(\zeta + \delta\eta(\zeta; x, t)\right), \tag{6.1}$$

where $|\delta| \ll 1$ and linearize (4.9) with respect to δ. When $\delta = 0$, (6.1) corresponds to a circle of radius a centred at the origin. We set

$$S_0 = \pi a^2,$$

and so require changes in cross-section area and centre of mass due to the perturbation δ to be zero.

First notice that

$$\left(f'(\zeta)\bar{f}'(1/\zeta)\right)^{-1/2} \sim \frac{1}{a} - \frac{\delta}{2a}(\eta'(\zeta) + \bar{\eta}'(1/\zeta)),$$

so from (4.6) we can read off $\mathscr{F}_{\pm}$ and hence obtain

$$\mathscr{G}(\zeta) \sim \frac{1}{a}\left(1 + \delta\frac{\eta'(0)}{2} - \delta\eta'(\zeta)\right). \tag{6.2}$$

Now considering (4.9) at order one (i.e. setting $\delta = 0$), and eliminating the $1/\zeta$ singularity on the left-hand side, we recover the usual mass-conservation result:

$$\mathrm{D}[a^2] = 0. \tag{6.3}$$

Then, considering the problem at order δ, we obtain the equation

$$\mathrm{D}\left[a^2\left(\bar{\eta}(1/\zeta) + \frac{\eta'(\zeta)}{\zeta}\right)\right] = \frac{\gamma^* a}{2}\frac{\partial}{\partial\zeta}\{\zeta\bar{\eta}(1/\zeta)\} + \{\text{function analytic in } |\zeta| < 1\}, \tag{6.4}$$

in which singularities must match within the unit disc.

As noted in § 4, if the cross-section possesses an axis of symmetry, then we can assume that $f(\zeta)$ is real whenever ζ is real, which allows us to pose the following form for η:

$$\eta(\zeta; x, t) = \sum_{k=3}^{\infty} d_k(x, t)\zeta^k, \tag{6.5}$$

where $d_k \in \mathbb{R}$. The constant term in the series is set to zero via the normalizing assumption $f(0) = 0$; preserving the area and centre of mass of the cross-section dictates that the coefficients of ζ and ζ^2 respectively be zero. Within the linear theory, (6.5) can be related directly to a polar-coordinates description of the cross-section:

$$r = a\left(1 + \sum_{k=2}^{\infty} d_{k+1}\cos(k\theta)\right).$$

Now we simply substitute (6.5) into (6.4) and equate the principal parts of the left- and right-hand sides at the pole $\zeta = 0$. The result is a set of decoupled equations for the coefficients d_k which, using the fact that $\mathrm{D}[a^2] = 0$, can be written in the form

$$\frac{1}{d_k}\frac{\mathscr{D}d_k}{\mathscr{D}t} = -\frac{\gamma^*(k-1)}{2a}. \tag{6.6}$$

This result could alternatively have been obtained by linearizing (4.14).

The circumference of the cross-section is given by

$$\Gamma_0 = \int_0^{2\pi} |f'(\mathrm{e}^{\mathrm{i}\theta})|\mathrm{d}\theta \sim 2\pi a\left\{1 + O\left(|\delta|^2\right)\right\}$$

(the $O(\delta)$ term integrates to zero) and so, within the linear theory the problem (3.3), (3.12) for S_0 and u_0 also decouples from (6.6). In summary, we have

$$\left(a^2\right)_t + \left(ua^2\right)_x = 0, \tag{6.7}$$

$$Re\, a^2\left(u_t + uu_x\right) = \left(3a^2u_x\right)_x + St\, a^2 + \gamma^* a_x \tag{6.8}$$

(for simplicity absorbing $\cos\beta$ into St) to determine a and u; then the evolution of the cross-section shape is given by (6.6).

This simple linearized system confirms that the predictions of the complex-variable analysis given in § 4 agree with what might have been anticipated on physical grounds. In particular, (6.6) shows that (i) a circular cross section is linearly stable, (ii) the decay rate increases as the cross-section shrinks (i.e. as a decreases), (iii) the higher modes decay faster.

7. Numerical results

We now present several numerical solutions of the fibre evolution for Example 1 of § 5. The same initial geometry is used for each of our calculations, this being a four-lobed cross-section, with a longitudinal sinusoidal perturbation imposed. Admittedly such initial geometry is contrived, to say the least; however this configuration serves well to illustrate the different effects of surface tension (the smoothing of the lobes to a circular cross-section), and axial inertia and gravity (the distortion of the initially regular sinusoidal profile). Several different scenarios are given, and the results are discussed further in § 10.1.

7.1. *Evolution with surface tension, but no axial inertia or gravity*

The simplest non-trivial case which has not yet been studied is obtained by setting $Re = 0$ and $St \cos\beta = 0$ in (5.5), corresponding to zero axial inertia and gravity respectively. That is, we are neglecting the component of gravity along the axis of the fibre. Gravity may still act perpendicular to the axis, which will not affect the evolution of the shape of the cross-section, but may influence the motion of the centre-line, and hence the twisting of the fibre, as can be seen from equations (3.14) and (3.15). We do not solve those problems in this paper. We assume in addition that the fibre is symmetric about its centre-plane $x = 0$, and that it is being stretched by means of rigid planes attached to its ends pulling at constant speeds in opposite directions, hence the boundary condition on u is just that it is constant at the endpoints. (An alternative equivalent scenario is that one end of the fibre is attached to a fixed rigid plate at $x = 0$ while the other end is being pulled in opposition.)

The numerical scheme is especially simple in this case. With $a(x,0)$, $b(x,0)$ given we solve the boundary-value problem (5.5) (just a second-order ODE) for $u(x,0)$. We can then step forward in time using (5.2) and (5.3) to find a and b at the next time-step. The scheme used here involves integration along characteristics, this method being particularly appropriate for conservative systems. After readjusting the mesh to account for the changing length of the fibre, we return to (5.5) and solve for u at this time-step, and so on.

Figure 4 shows the evolution of the cross-section of a fibre being pulled from each end with unit speed, for an initial fibre shape given by

$$a(x,0) = 0.2(1 + 0.1\cos(5\pi x)), \quad b(x,0) = 0.95 \quad (0 < x < 1).$$

The initial data $a(x,0)$ describes the longitudinal variation. As commented earlier, the sinusoidal dependence is chosen for illustrative purposes only, and may easily be changed to describe a more physically realistic fibre. The parameter n is taken to be 5 in the conformal map, giving a four-lobed cross-section. The fact that $b(x,0)$ is close to unity means that these four lobes are initially very pronounced. Only one half of the fibre (in $x > 0$) is shown, and the time-steps illustrated are $t = 0, 0.3, 0.75$. Note that the true evolution of the fibre will have the centre-line motion and twisting as determined by (3.14) and (3.15) superimposed onto this motion, a comment which applies to all of our numerical solutions.

7.2. *Evolution with surface tension and axial inertia, but no axial gravity*

It is also not difficult to solve for the case of non-zero Reynolds number in (5.5). In this case however a slightly different approach is needed; in particular, we must now postulate some kind of start-up procedure for the fibre-drawing, because equation (5.5) now has explicit time dependence. We consider the simple scenario in which the fibre (again symmetric about the plane $x = 0$) is initially at rest, and its ends are

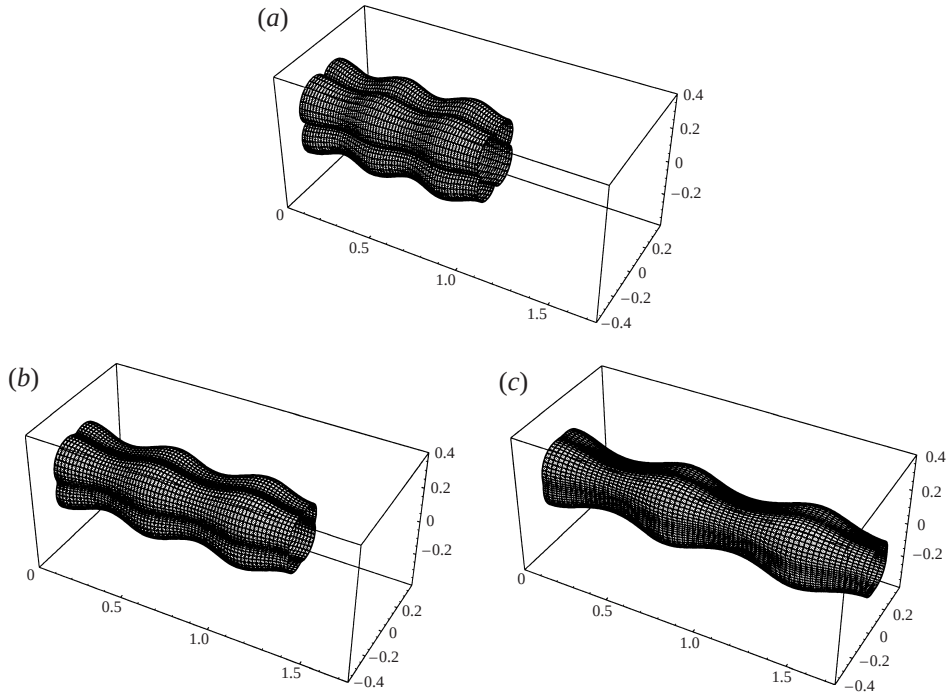

FIGURE 4. Evolution of a viscous fibre pulled with constant speed from each end, with no axial inertia or gravity. The configuration is symmetric about the plane $x = 0$, hence only half the fibre is shown. The value of the surface tension parameter γ^* is 0.04π.

accelerated smoothly from rest according to the law $u_i^* = \pm t^2$ ($t \geqslant 0$) (in the notation of (2.3)).

Again the initial fibre shape $a(x, 0)$, $b(x, 0)$ is prescribed. We step forwards in time in equations (5.2) and (5.3) using a simple upwind scheme (in conservation form) to solve for a and b at the next time-step. After a mesh readjustment to account for the changed fibre length, we use these values to solve the parabolic PDE (5.5) for u at this time-step, using a semi-implicit method. With the new values for u we return to (5.2) and (5.3) and again step forwards in time, and so on.

Figure 5 shows the evolution of a fibre with this start-up procedure for the same initial geometry as § 7.1 (i.e. as shown in figure 4*a*), at times $t = 1$, 1.4.

7.3. *Evolution with surface tension, axial inertia, and axial gravity*

This is a simple extension of the example in § 7.2 above, and we may solve for the same start-up procedure and geometry. However, the fibre cannot now be symmetric about the plane $x = 0$ because gravity acts only in one direction along the fibre axis. Thus in this example we interpret $x = 0$ as a fixed stationary plate to which one end of the fibre is attached, the other end being pulled away from this plate. Gravity may act either towards or away from the plate, and an example of each case is shown in figure 6. In this figure, (*a*) and (*b*) show the later stages for evolution in which the right-hand end of the fibre is being pulled to the right, and gravity acts along the fibre axis to the left. This may be thought of as pulling a fibre upwards from one end, the other end being stuck to a horizontal table. In (*c*) and (*d*) of figure 6 gravity acts along the fibre axis to the right, which we may think of as pulling a fibre down from a horizontal ceiling. In either case, the times shown are $t = 1$, 1.3.

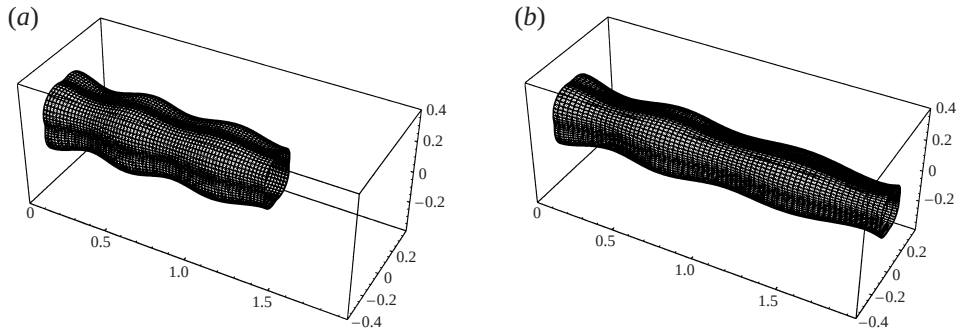

FIGURE 5. Evolution of fibres with surface tension and axial inertia. The value of the surface tension parameter γ^* is 0.02π, $Re = 1.0$, and $St\cos\beta = 0$.

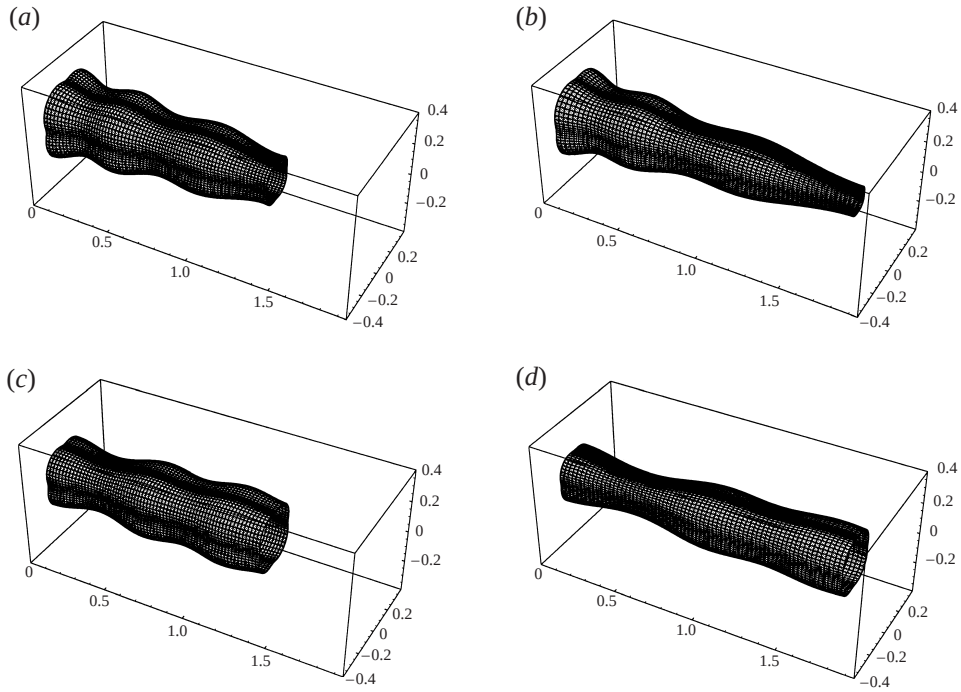

FIGURE 6. Evolution of fibres with surface tension, axial inertia, and axial gravity. Gravity acts to the left along the fibre axis in (*a*) and (*b*), and to the right in (*c*) and (*d*). The surface tension parameter is $\gamma^* = 0.02\pi$, and $Re = 1.0$ for both cases. In (a, b) $St\cos\beta = -1.5$, and in (c, d) $St\cos\beta = +1.5$.

8. Transformation to Lagrangian variables

We have seen in § 7 that for many interesting initial shapes, the system of partial differential equations governing the evolution of the fibre can readily be solved numerically (certainly more readily than the three-dimensional Navier–Stokes equations!). However, without running very many such simulations one cannot deduce much general qualitative information from purely numerical results. Moreover we have already noted that the complex-variable formulation of the evolution problem (4.9), although elegant, is not particularly helpful when seeking insight into the be-

haviour of solutions in general. For example, in §6 we showed that stretching and sintering decouple for nearly circular fibres, but otherwise the relation between the two processes is far from clear from (4.9) alone.†

In this Section we use a coordinate transformation to clarify the mutual influence between stretching and sintering. Dewynne *et al.* (1994) used suitably defined Lagrangian variables to simplify the problem ((3.15) with $\gamma^* = 0$) for the twist of the fibre. Although in this paper we do not attempt to solve for the twist, we find that a similar transformation can be used to reduce the leading-order cross-flow problem (3.1*b*, *c*, *d*) with boundary conditions (3.1*e*, *g*, *h*) to the classical two-dimensional Stokes flow problem.

The first step is to transform to coordinates that convect with the fluid in the x-direction, and (i) translate with the centre-line $\boldsymbol{r}^*$, (ii) scale with the size of the cross-section and (iii) rotate with the mean angular velocity of the cross-section, in the (y, z)-plane. Thus we set (dropping the zero subscripts throughout)

$$t = \tilde{t}, \tag{8.1a}$$

$$x = X(\tilde{x}, \tilde{t}), \tag{8.1b}$$

$$y - y^* = \sqrt{S}(\tilde{y}\cos\alpha + \tilde{z}\sin\alpha), \tag{8.1c}$$

$$z - z^* = \sqrt{S}(\tilde{z}\cos\alpha - \tilde{y}\sin\alpha), \tag{8.1d}$$

where the functions $X(\tilde{x}, \tilde{t})$ and $\alpha(\tilde{x}, \tilde{t})$ are given by

$$\frac{\partial X}{\partial \tilde{t}} = u(X, \tilde{t}), \quad X(\tilde{x}, 0) = \tilde{x}, \tag{8.2a}$$

$$\frac{\partial \alpha}{\partial \tilde{t}} = c(X, \tilde{t}), \quad \alpha(\tilde{x}, 0) = 0, \tag{8.2b}$$

with c as defined in (3.5). This is similar to the transformation employed in §4; for example the definition of α is identical to (4.5). Notice that the rescaling of y and z means that in the transformed $(\tilde{y}, \tilde{z})$-plane, the cross-section (say $\tilde{S}$) always has unit area.

When transforming the dependent variables to these rotating coordinates, we simultaneously subtract the zero-surface-tension eigensolution (3.4) and rescale the velocity and pressure, thus

$$p = P_{ZST} + \frac{\gamma^*}{\sqrt{S}}\tilde{p}, \tag{8.3a}$$

$$v = V_{ZST} + \gamma^*(\tilde{v}\cos\alpha + \tilde{w}\sin\alpha), \tag{8.3b}$$

$$w = W_{ZST} + \gamma^*(\tilde{w}\cos\alpha - \tilde{v}\sin\alpha). \tag{8.3c}$$

As a result of these definitions, $\tilde{v}$ and $\tilde{w}$ satisfy

$$\iint_S \begin{pmatrix} \tilde{v} \\ \tilde{w} \end{pmatrix} \mathrm{d}\tilde{y}\,\mathrm{d}\tilde{z} = \mathbf{0}, \quad \iint_S (\tilde{y}\tilde{w} - \tilde{z}\tilde{v})\,\mathrm{d}\tilde{y}\,\mathrm{d}\tilde{z} = 0, \tag{8.4}$$

that is, with respect to the tilded variables, the cross-section has no linear or angular momentum.

† We are grateful to a referee of the first draft of this paper for bringing this point to our attention.

Substituting (8.1)–(8.3) into the cross-flow problem (3.1b, e, g, h) we find that

$$\tilde{v}_{\tilde{y}} + \tilde{w}_{\tilde{z}} = 0, \tag{8.5a}$$

$$\tilde{v}_{\tilde{y}\tilde{y}} + \tilde{v}_{\tilde{z}\tilde{z}} = \tilde{p}_{\tilde{y}}, \tag{8.5b}$$

$$\tilde{w}_{\tilde{y}\tilde{y}} + \tilde{w}_{\tilde{z}\tilde{z}} = \tilde{p}_{\tilde{z}}, \tag{8.5c}$$

$$(\sqrt{S}/\gamma^*)G_{\tilde{t}} + \tilde{v}G_{\tilde{y}} + \tilde{w}G_{\tilde{z}} = 0 \quad \text{on } G = 0, \tag{8.5d}$$

$$G_{\tilde{y}}(-\tilde{p} + 2\tilde{v}_{\tilde{y}}) + G_{\tilde{z}}(\tilde{v}_{\tilde{z}} + \tilde{w}_{\tilde{y}}) = -\tilde{\kappa}G_{\tilde{y}} \quad \text{on } G = 0, \tag{8.5e}$$

$$G_{\tilde{y}}(\tilde{v}_{\tilde{z}} + \tilde{w}_{\tilde{y}}) + G_{\tilde{z}}(-\tilde{p} + 2\tilde{w}_z) = -\tilde{\kappa}G_{\tilde{z}} \quad \text{on } G = 0. \tag{8.5f}$$

This can now be transformed into the two-dimensional Stokes flow problem (with unit surface tension) by defining the *reduced time* τ:

$$\tau = \gamma^* \int_0^{\tilde{t}} \frac{\mathrm{d}\tilde{t}}{\sqrt{S}}. \tag{8.6}$$

This has some striking, although perhaps with hindsight not unexpected, implications. Suppose at time zero we pick a particular cross-section of the fibre; then, as the fibre evolves over time we follow this section as it convects, translates and rotates. What we have shown is that its shape evolves according to a classical two-dimensional Stokes flow free-boundary problem. We can solve this problem, either numerically or analytically (see § 4) 'once and for all', starting from the given initial shape of the cross-section. From such a calculation we can obtain the circumference $\tilde{\Gamma}(\tau)$. Finally, this can be transformed back to the physical (but still Lagrangian) plane via

$$\Gamma(\tilde{x}, \tilde{t}) = \sqrt{S}\,\tilde{\Gamma}(\tau),$$

with τ given by (8.6). By performing this procedure for each Lagrangian cross-section (i.e. for each $\tilde{x}$) we obtain the relation between Γ and S required to close the system (3.3), (3.12) for S and u.

In summary, we have succeeded in partially decoupling stretching from sintering. Stretching only affects sintering by decreasing the cross-section area S, which accelerates sintering through (8.6). Conversely the effect of sintering on the stretching problem comes in only through the function $\tilde{\Gamma}(\tau)$, which satisfies a canonical two-dimensional Stokes flow problem.

We verify this result in figure 7, for the numerical solution shown in figure 4. We could have used any of the solutions presented in § 7, but the numerical method applied in this case (effectively using Lagrangian variables) made it the most convenient. We pick two material cross-sections with different initial areas and plot the evolution of b (which parametrizes the shape of the cross-section) with time in figure 7(a). It is clear that the shape evolves faster for one cross-section (the thinner one) than for the other. However, in figure 7(b) we plot both versus reduced time τ, as well as the evolution of b for the two-dimensional Stokes flow problem. The seemingly exact agreement between the three curves confirms both the theory of this Section and the accuracy of our numerical solution.

9. Motion of the centre-line, and the twisting problem

We now briefly outline, but do not attempt to solve, the problems that determine in principle the lateral motion and twist of the fibre. It is instructive to compare these with the corresponding zero-surface-tension problems obtained by Dewynne *et*

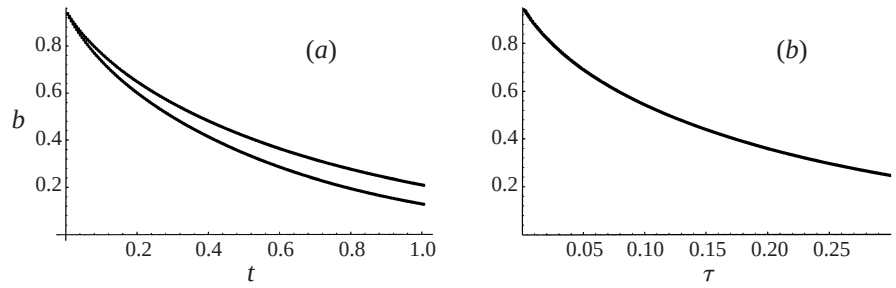

FIGURE 7. The shape parameter b versus time for the numerical solution shown in figure 4; (a) shows the evolution for two cross-sections with different initial areas. In (b) the two are plotted against reduced time τ, along with the solution of the two-dimensional Stokes flow problem; all three graphs collapse onto one curve.

al. (1994). First consider the axial force balance (3.12), which was obtained from the solvability condition for the Neumann problem (3.10) for the first-order axial velocity u_1. If γ^* is set to zero, (3.12) and (3.3) constitute a closed system that determines S_0 and u_0. However when surface tension is included, more information is required to close the problem, namely the evolution of the shape of the fibre cross-section. To determine this, we have to solve for the leading-order cross-flow, i.e. v_0 and w_0.

Now consider the lateral force balance (3.14), which was obtained from the solvability condition for the problem (3.13b, e) for the first-order cross-flow (v_1, w_1). Again, if $\gamma^* = 0$, once u_0 is known (from the solution of (3.3) and (3.12)), (3.14) determines the evolution of the centre-line $\boldsymbol{r}^*$. For non-zero surface tension, the analysis of § 4 allows us to determine the leading-order shape of the cross-section as a function of x and t. Thus, all the integrals except the last on the right-hand side of (3.14) can be calculated (this may be facilitated by use of the complex-variable description of S_0 introduced in § 4). However, to evaluate the final integral we need to know κ_1; that is we must determine the first-order shape of the cross-section. Since this evolves according to the first-order transverse velocities, we must solve for the first-order cross-flow (v_1, w_1): the solvability condition is not sufficient to obtain a closed problem for the motion of the centre-line. It is this additional complication that makes (3.14) so much more difficult to solve when surface tension is included.

The same difficulty arises in the problem (3.15) for the twist of the fibre. Here, even when $\gamma^* = 0$ one must solve the Neumann problem (3.10) for u_1, but since in this limit the shape of the cross-section is fixed, if one transforms to a Lagrangian frame one need solve this problem only once – see Dewynne *et al.* (1994). Even when surface tension is included, so that the cross-section evolves in time and space, our complex-variable description of S_0 allows in principle all except the final integral in (3.15) to be determined in terms of the x- and t-dependent conformal map f. Thus it is again the appearance of κ_1 in the final term that seriously hinders any further analytical progress.

10. Discussion

We have derived leading-order equations governing the evolution of an axially stretched slender viscous fibre under surface tension, gravity and inertia. This represents a generalisation of earlier work by Dewynne *et al.* (1994) in which surface tension was ignored. A greatly simplifying property of the zero-surface-tension solu-

tion is that each cross-section of the fibre retains its shape. We presented a method whereby the considerable extra complication that arises when surface tension is included, and this property is lost, may be tackled using complex-variable techniques previously applied to purely two-dimensional Stokes flow by Hopper (1990) and Richardson (1992). Thus for many shapes of potential practical interest, one can obtain a relatively simple system of partial differential equations in one space and one time variable, governing the evolution of the axial velocity u, the cross-sectional area S, and one or more parameters describing the shape of the cross-section. This represents a huge simplification of the full Navier–Stokes free-boundary problem.

In § 8 we showed that in fact the problem for the cross-flow (that is flow perpendicular to the axis of the fibre) can, by a suitable Lagrangian coordinate transformation, be reduced to exactly the two-dimensional Stokes flow problem. This enabled us to infer some interesting general properties of the coupling between stretching and sintering. We note that this offers an alternative route to the application of the techniques from Hopper (1990) and Richardson (1992). However, we opted for the direct conversion of the cross-flow problem into complex-variable form rather than the lengthier transformation Eulerian → Lagrangian → complex-variable.

We found that surface tension effects make it considerably harder to determine the fibre centre-line and twist, and for that reason we did not attempt to do so in this paper. It is fortunate that the problems decouple; that is, the fact that we have been (thus far) unable to solve for the centre-line and twist does not prevent us from finding the evolution of the cross-section shape, since in many applications it is this shape, in particular S and the degree to which sintering has occurred, that is of paramount importance.

10.1. *Comments on numerical results*

The initial configurations used for our numerical calculations are somewhat idealized and, in particular, the axial variations are greatly exaggerated compared to what might be expected in practical situations. This allows us to highlight some physically important features of the fibre evolution, including the following.

It was found numerically that the sintering process takes place extremely rapidly. That is, the evolution of the cross-section towards a circular shape appears to be significantly accelerated by axial stretching (compared with the planar solutions of Richardson 1992 for example). Hence small values of the dimensionless surface tension coefficient γ^* were chosen so that the sintering could be observed over an appreciable timescale. This does suggest that some processes might be decomposed into an initial rapid sintering stage, in which stretching and twisting are negligible, followed by a stretching/twisting phase in which the fibre has an effectively circular cross-section. Such an approach, if valid, would further simplify the solution procedure.

As is typical in fibre-drawing processes, the thinnest points in the initial configuration tend to neck first. Since surface tension becomes increasingly important as S decreases, one can observe that, while the thinnest points rapidly approach a circular shape, the sintering of the fatter portions of the fibre lags behind (figure 7*a*).

Since as just noted, the cross-section rapidly becomes circular as S becomes small, the local behaviour for small S can be inferred from axisymmetric calculations. These show that with surface tension (in contrast to the zero-surface-tension limit considered by Dewynne *et al.* 1994), there are solutions in which $S \to 0$, i.e. the fibre breaks up, in finite time – see Eggers (1993).

Moreover, in glass-fibre sintering processes, the parameters Re and St are often small enough that inertia and gravity may safely be neglected. Again, we have used

relatively (maybe unphysically) large values in our calculations to emphasize the influence of each of these effects, and can deduce the following.

With neither inertia nor gravity, any axial symmetries in the initial configuration are preserved by the stretching process (figure 4).

This symmetry is lost when inertia is significant. In figure 5 one can observe the diffusion of momentum through the fibre, starting at the moving end.

The most important effect of inertia is that more of the fluid in the fibre is 'left behind' in the centre as the ends are stretched, with the pulled ends 'thinning out'. If this is undesirable, the ends must be pulled slowly, giving a small (axial) Reynolds number, and hence negligible inertial effects.

Not surprisingly, gravity similarly induces loss of symmetry, with fluid tending to 'pile up' at the lower end. This effect may be eliminated by stretching the fibre in a horizontal plane.

If one wishes to make the fibre as uniform as possible, the effects of inertia and gravity can be made partially to cancel each other out if the fibre is stretched downwards – see figure 6 (a, b) ((c) and (d) in this figure show the opposite situation in which the effects combine, giving a highly non-uniform fibre).

Sometimes these effects may be desired – for example, glass artists can utilize such phenomena to create tapering structures.

In this paper we have drawn heavily on the previous literature on two-dimensional viscous sintering. This has received much attention because of the remarkable exact solutions that can be found using complex-variable techniques. In practice, of course there is no such thing as a purely two-dimensional flow, and we have shown how the same ideas and techniques can be applied to a more physically realistic three-dimensional (albeit slowly varying) geometry. A possible application of our work is to quantify three-dimensional effects in experiments on the sintering of finite cylinders.

P. D. H. gratefully acknowledges the financial support of a Junior Research Fellowship from Christ Church, Oxford. L. J. C. was in receipt of a Postdoctoral Research Fellowship funded by the Israel Council for higher Education, at the Technion, Haifa.

Appendix A. The axial force balance

First we show how to obtain the axial force balance (3.12) by substituting the right-hand side of the Neumann problem (3.10) into the identity (3.11). When performing the integrations, we use the transport theorem (2.6b) and the divergence theorem on the right-hand side of (3.10b) and then substitute for v_0 from (3.1d) to obtain

$$(3S_0u_{0_x})_x - ReS_0(u_{0_t} + u_0u_{0_x}) + S_0St\cos\beta = -\frac{1}{2}\frac{\partial}{\partial x}\int\int_{S_0}\hat{\nabla}^2\mathscr{A}\,\mathrm{d}y\,\mathrm{d}z + \gamma^*\oint_{\partial S_0}\frac{\kappa_0 G_{0_x}\,\mathrm{d}s}{\sqrt{G_{0_y}^2 + G_{0_z}^2}}. \tag{A 1}$$

For the first integral we simply apply the divergence theorem followed by the boundary condition (3.8) satisfied by $\mathscr{A}$, which gives

$$\int\int_{S_0}\hat{\nabla}^2\mathscr{A}\,\mathrm{d}y\,\mathrm{d}z = -\gamma^*\oint_{\partial S_0}\mathrm{d}s = -\gamma^*\Gamma_0, \tag{A 2}$$

where as in the text Γ_0 denotes the circumference of the cross-section.

The second integral on the right-hand side of (A 1) is most readily simplified by

writing the free surface in parametric form (using arclength s as the parameter):

$$\begin{pmatrix} y \\ z \end{pmatrix} = \begin{pmatrix} Y(s;x,t) \\ Z(s;x,t) \end{pmatrix}.$$

In this notation,

$$\oint_{\partial S_0} \frac{\kappa_0 G_{0_x}\,\mathrm{d}s}{\sqrt{G_{0_y}^2+G_{0_z}^2}} = \int_0^{\Gamma_0} \kappa_0(Y_sZ_x - Z_sY_x)\,\mathrm{d}s = \int_0^{\Gamma_0} (Y_{ss}Y_x + Z_{ss}Z_x)\,\mathrm{d}s$$

$$= \int_0^{\Gamma_0} (Y_sY_x + Z_sZ_x)_s\,\mathrm{d}s = [Y_sY_x + Z_sZ_x]_0^{\Gamma_0}, \tag{A 3}$$

using successively the Serret–Frenet formulae and the identity

$$Y_s^2 + Z_s^2 \equiv 1 \quad \Rightarrow \quad Y_sY_{sx} + Z_sZ_{sx} \equiv 0.$$

Now, Y, Z and their s-derivatives are periodic, with period Γ_0, but the x-derivatives are not, for

$$Y(\Gamma_0;x,t) = Y(0;x,t) \quad \Rightarrow \quad Y_x(\Gamma_0;x,t) - Y_x(0;x,t) = -\Gamma_{0_x} Y_s(0;x,t),$$

and similarly for Z. Thus, substituting this into (A 3) we finally obtain

$$\oint_{\partial S_0} \frac{\kappa_0 G_{0_x}\,\mathrm{d}s}{\sqrt{G_{0_y}^2+G_{0_z}^2}} = -\frac{\partial \Gamma_0}{\partial x}. \tag{A 4}$$

Then (3.12) follows trivially from (A 1).

Appendix B. The transverse force balance

Now we derive the transverse force balance (3.14), which results from integration of (3.13b, c) over the cross-section, by establishing a series of simpler results. We start by applying the transport equations (2.6a, b) and kinematic boundary condition (3.1e) to obtain

$$\frac{\mathscr{D}}{\mathscr{D}t}\left(S_0 y^*\right) = -\oint_{\partial S_0} \frac{y(G_{0_t} + u_0 G_{0_x})\,\mathrm{d}s}{\sqrt{G_{0_y}^2+G_{0_z}^2}} = \oint_{\partial S_0} \frac{y(v_0 G_{0_y} + w_0 G_{0_z})\,\mathrm{d}s}{\sqrt{G_{0_y}^2+G_{0_z}^2}},$$

where $\mathscr{D}/\mathscr{D}t = \partial/\partial t + u_0\partial/\partial x$ is the usual convective derivative. Then we apply the divergence theorem to the right-hand side and substitute for v_0 and w_0 from (3.1d):

$$\frac{\mathscr{D}}{\mathscr{D}t}\left(S_0 y^*\right) = \iint_{S_0} v_0\,\mathrm{d}y\,\mathrm{d}z - y^* S_0 u_{0_x}.$$

An analogous result holds for z^*, and these may be rearranged to the useful identity

$$\frac{\mathscr{D}\boldsymbol{r}^*}{\mathscr{D}t} = \frac{1}{S_0}\iint_{S_0} \begin{pmatrix} v_0 \\ w_0 \end{pmatrix} \mathrm{d}y\,\mathrm{d}z. \tag{B 1}$$

Similarly, consideration of

$$\frac{\mathscr{D}}{\mathscr{D}t}\iint_{S_0} v_0\,\mathrm{d}y\,\mathrm{d}z$$

leads to the identity

$$\frac{\mathscr{D}}{\mathscr{D}t}\left[\frac{1}{S_0}\iint_{S_0}\begin{pmatrix} v_0 \\ w_0 \end{pmatrix}\mathrm{d}y\,\mathrm{d}z\right] = \frac{1}{S_0}\iint_{S_0}\begin{pmatrix} v_{0_t}+u_0v_{0_x}+v_0v_{0_y}+w_0v_{0_z} \\ w_{0_t}+u_0w_{0_x}+v_0w_{0_y}+w_0w_{0_z} \end{pmatrix}\mathrm{d}y\,\mathrm{d}z. \tag{B 2}$$

This takes care of the left-hand sides of (3.13*b*, *c*). For the right-hand sides we rearrange and use the divergence theorem to obtain

$$\begin{aligned}\iint_{S_0}&(-p_{1_y}+v_{0_{xx}}+v_{1_{yy}}+v_{1_{zz}})\,\mathrm{d}y\,\mathrm{d}z\\ &=\iint_{S_0}(-p_1+2v_{1_y})_y+(v_{1_z}+w_{1_y})_z+(u_{1_y}+v_{0_x})_x\,\mathrm{d}y\,\mathrm{d}z\\ &=\iint(u_{1_y}+v_{0_x})_x\,\mathrm{d}y\,\mathrm{d}z+\oint_{\partial S_0}\frac{(-p_1+2v_{1_y})G_{0_y}+(v_{1_z}+w_{1_y})G_{0_z}\,\mathrm{d}s}{\sqrt{G_{0_y}^2+G_{0_z}^2}}.\end{aligned}$$

Now we substitute from (3.13*d*) into the boundary integral and use the transport theorem (2.6*b*), resulting in

$$\iint_{S_0}(-p_{1_y}+v_{0_{xx}}+v_{1_{yy}}+v_{1_{zz}})\,\mathrm{d}y\,\mathrm{d}z=\frac{\partial}{\partial x}\iint_{S_0}(u_{1_y}+v_{0_x})\,\mathrm{d}y\,\mathrm{d}z-\gamma^*\oint_{\partial S_0}\frac{\kappa_1 G_{0_y}\,\mathrm{d}s}{\sqrt{G_{0_y}^2+G_{0_z}^2}}.$$

An analogous result holds for the z-component, and so integration of (3.13*b*, *c*) over S_0 and use of (B 1), (B 2) leads to

$$ReS_0\frac{\mathscr{D}^2\boldsymbol{r}^*}{\mathscr{D}t^2}=\frac{S_0St\sin\beta}{\epsilon}\boldsymbol{j}+\frac{\partial}{\partial x}\iint_{S_0}\begin{pmatrix} u_{1_y}+v_{0_x} \\ u_{1_z}+w_{0_x}\end{pmatrix}\mathrm{d}y\,\mathrm{d}z-\gamma^*\oint_{\partial S_0}\kappa_1\hat{\boldsymbol{n}}\,\mathrm{d}s, \tag{B 3}$$

where $\boldsymbol{j}=(1,0)^T$ is the unit vector in the y-direction.

Use of the transport theorem (2.6*c*), followed by substitution from (3.10) leads to

$$\begin{aligned}\iint_{S_0}u_{1_y}\mathrm{d}y\,\mathrm{d}z=\oint_{\partial S_0}&\frac{[G_{0_x}(p_0-2u_{0_x}-\gamma^*\kappa_0)-G_{0_y}v_{0_x}-G_{0_z}w_{0_x}]y\,\mathrm{d}s}{\sqrt{G_{0_y}^2+G_{0_z}^2}}\\ &+y^*S_0\left[St\cos\beta+u_{0_{xx}}-Re(u_{0_t}+u_0u_{0_x})\right]-\iint_{S_0}yp_{0_x}\mathrm{d}y\,\mathrm{d}z.\end{aligned}$$

We use (2.6*b*) on the first part of the boundary integral and the divergence theorem on the rest before substituting from (3.1*d*), to obtain

$$\begin{aligned}\iint_{S_0}(u_{1_y}+v_{0_x})\mathrm{d}y\,\mathrm{d}z=&-\frac{\partial}{\partial x}\iint_{S_0}yp_0\,\mathrm{d}y\,\mathrm{d}z-\gamma^*\oint_{\partial S_0}\frac{\kappa_0G_{0_x}y\,\mathrm{d}s}{\sqrt{G_{0_y}^2+G_{0_z}^2}}\\ &+2\left(S_0y^*u_{0_x}\right)_x-y^*S_0\left[Re(u_{0_t}+u_0u_{0_x})-St\cos\beta\right].\end{aligned} \tag{B 4}$$

But p_0 is given in terms of the Airy stress function $\mathscr{A}$ by (3.9*a*). Thus we can apply (2.6*c*) and then use the boundary conditions (3.8) satisfied by $\mathscr{A}$ to simplify the resulting integrals, and arrive at the result

$$\iint_{S_0}yp_0\,\mathrm{d}y\,\mathrm{d}z=-S_0y^*u_{0_x}+\frac{\gamma^*}{2}\oint_{\partial S_0}y\,\mathrm{d}s. \tag{B 5}$$

We substitute (B 5) into (B 4) and rearrange, using the axial force balance (3.12), to

end up with

$$\iint_{S_0} \begin{pmatrix} u_{1_y} + v_{0_x} \\ u_{1_z} + w_{0_x} \end{pmatrix} \mathrm{d}y\,\mathrm{d}z = \boldsymbol{r}_x^* \left(3S_0 u_{0_x} - \frac{\gamma^* \Gamma_0}{2} \right) - \gamma^* \oint_{\partial S_0} \frac{(\boldsymbol{r} - \boldsymbol{r}^*)\kappa_0 G_{0_x}\,\mathrm{d}s}{\sqrt{G_{0_y}^2 + G_{0_z}^2}} - \frac{\gamma^*}{2} \frac{\partial}{\partial x} \oint_{\partial S_0} (\boldsymbol{r} - \boldsymbol{r}^*)\ \mathrm{d}s. \quad \text{(B 6)}$$

It is then a simple matter to substitute (B 6) into (B 3) and rearrange, once again using (3.12) to arrive at the transverse force balance (3.14).

Appendix C. The twist equation

The equation (3.15) for the twist of the fibre about its centre-line is obtained by integrating $\{y \times (3.13c) - z \times (3.13b)\}$ over S_0. The steps involved are similar to those used in Appendix B, so we omit more of the details. First, the transport theorems (2.6*a*, *b*), followed by the kinematic boundary condition (3.1*e*) give rise to the identity

$$\frac{1}{S_0} \iint_{S_0} y(w_{0_t} + u_0 w_{0_x} + v_0 w_{0_y} + w_0 w_{0_z}) - z(v_{0_t} + u_0 v_{0_x} + v_0 v_{0_y} + w_0 v_{0_z})\,\mathrm{d}y\,\mathrm{d}z = \frac{\mathscr{D}}{\mathscr{D}t} \left\{ \frac{1}{S_0} \iint_{S_0} y w_0 - z v_0 \mathrm{d}y\,\mathrm{d}z \right\}. \quad \text{(C 1)}$$

Secondly, a rearrangement of the right-hand side (as in Appendix B), followed by the divergence theorem and then use of the boundary conditions (3.13*d*, *e*) leads to

$$\iint_{S_0} y(-p_{1_z} + w_{0_{zz}} + w_{1_{yy}} + w_{1_{zz}}) - z(-p_{1_y} + v_{0_{zz}} + v_{1_{yy}} + v_{1_{zz}})\,\mathrm{d}y\,\mathrm{d}z = \frac{\partial}{\partial x} \iint_{S_0} y(w_{0_x} + u_{1_z}) - z(v_{0_x} + u_{1_y})\,\mathrm{d}y\,\mathrm{d}z + \gamma^* \oint_{\partial S_0} \frac{\kappa_1 \left(z G_{0_y} - y G_{0_z} \right)\ \mathrm{d}s}{\sqrt{G_{0_y}^2 + G_{0_z}^2}}. \quad \text{(C 2)}$$

REFERENCES

Byrd, P. F. & Friedman, M. D. 1971 *Handbook of Elliptic Integrals for Engineers and Scientists.* Springer.

Cummings, L. J., Howison, S. D. & King, J. R. 1997 Conserved quantities in Stokes flow with free surfaces. *Phys. Fluids* **9**, 477–480.

Dewynne, J. N., Howell, P. D. & Wilmott, P. 1994 Slender viscous fibres with inertia and gravity. *Q. J. Mech. Appl. Maths* **47**, 541–555.

Dewynne, J. N., Ockendon, J. R. & Wilmott, P. 1992 A systematic derivation of the leading-order equations for extensional flows in slender geometries. *J. Fluid Mech.* **244**, 323–338.

Eggers, J. 1993 Universal pinching of 3D axisymmetric free-surface flow. *Phys. Rev. Lett.* **71**, 3458–3460.

Eggers, J. & Dupont, T. F. 1994 Drop formation in a one-dimensional approximation of the Navier–Stokes equation. *J. Fluid Mech.* **262**, 205–221.

Gradshteyn, I. S. & Ryzhik, I. M. 1980 *Table of Integrals, Series and Products* (corrected and enlarged edition). Academic.

Hopper, R. W. 1990 Plane Stokes flow driven by capillarity on a free surface. *J. Fluid Mech.* **213**, 349–375.

Howell, P. D. 1994 Extensional thin layer flows. D.Phil. thesis, University of Oxford.

HOWISON, S. D. & RICHARDSON, S. 1995 Cusp development in free boundaries, and two-dimensional slow viscous flows. *Eur. J. Appl. Maths* **6**, 441–454.

NEHARI, Z. 1975 *Conformal Mapping*. Dover.

RICHARDSON, S. 1992 Two-dimensional slow viscous flows with time-dependent free boundaries driven by surface tension. *Eur. J. Appl. Maths* **3**, 193–207.

SCHULTZ, W. W. & DAVIS, S. H. 1982 One-dimensional liquid fibres. *J. Rheology* **26**, 331–345.

TING, L. & KELLER, J. B. 1990 Slender jets and sheets with surface tension. *SIAM J. Appl. Maths* **50**, 1533–1546.